Advances in Environmental and Life Sciences 4(1) (2023) 11-22

Contents lists available at Egyptian Knowledge Bank

Advances in Environmental and Life Sciences

journal homepage: https://aels.journals.ekb.eg

Fluorescence Detection of Ascorbic Acid in Pharmaceutical Ingredients

Adel Sayed Orabi, Mohamed Magdy El-Fiky*, Ibrahim Ahmed Ibrahim, Abbas Mamdoh Abbas

Chemistry Department, Faculty of Science, Suez Canal University, 41522, Ismailia, Egypt

Abstract

A new complex was prepared from nicotinic acid and terbium chloride (Nic-Tb) and characterized using sophisticated techniques (CHN, FT-IR, UV ,TGA and DTA thermal techniques). The prepared complex determined the ascorbic acid concentration in the pharmaceutical ingredient. The luminescence intensity of the probe decreases as the concentrations of the ascorbic acid increase. At different temperatures, Stern–Volmer studies indicate a dynamic quenching mechanism. The calculation of the thermodynamic parameters ((ΔS^o, ΔH^o, and ΔG^o) and binding constants (K) of the Ascorbic acid-probe complex interaction revealed a spontaneous hydrophobic interaction. The specified range was found to be in the range of 1×10^{-5} – 1×10^{-4} M. The recovery values were 97.6 - 98.89. The fluorescence probe's quenching mechanism was collisional (dynamic), as demonstrated by the experiments. The interaction by electrostatic forces is shown by the thermodynamic parameter values.The limit of detection was found to be equal to 9.1 μM and the quantitation limit was 28 μM.

Keywords: Ascorbic Acid, Fluorescence, Terbium, Quenching, pharmaceuticals

1. Introduction

The body needs vitamin C for regular physiological functions, It helps in the metabolism of folic acid, tryptophan and tyrosine. It helps to reduce blood cholesterol and provides for the creation of amino acids that regulate the nervous system. It is necessary for injury treatment and tissue growth. It helps in the creation of neurotransmitters and improves iron absorption in the stomach. Being an antioxidant, it protects the body from the free radicals and their poisons dangerous effects. Extra-large doses of vitamin C are treated and inhibit many disorders like cataracts, diabetes, glaucoma, atherosclerosis, macular degeneration, cancer, stroke and heart diseases. The insufficiency of this vitamin is able to lead to scurvy ,anaemia, muscle degeneration, bleeding gums, poor wound healing, capillary haemorrhaging, atherosclerotic plaques, and neurotic disturbances. [1, 2]. In the food industry, as an antioxidant, ascorbic acid (**figure 1**) is widely utilised to stop colour or taste changes. Nevertheless, it is crucial to create analytical techniques for ascorbic acid) quantification in the presence of interfering species.

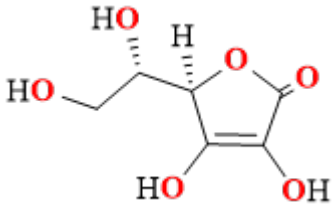

Figure 1: Structure of AscorbicAcid (AA)

Sensor based on fluorescence technique is the most one of imaging agents are used in drug discovery. Such sensors made it possible to learn more about enzymes' function and control at the cellular level. A receptor is used to install one or more fluorescent-based probes (either chemically, enzymatically, or genetically) into fluorescent biosensors, which are small platforms. A fluorescence

* Corresponding author.
Email address: mohamed_magdy@suez.edu.eg (Mohamed Magdy El-Fiky)

doi 10.21608/AELS.2023.188537.1028

Received : 24 February 2023, Revised : 3 March 2023
Accepted: 21 March 2023, Published: 21 March 2023

signal that can be easily detected and measured is produced when a specific analyte is detected by the receptor. [3, 4]. Fluorescent biosensors can investigate metabolites, ions, and protein biomarkers with good sensitivity [5–8]. Fluorescent sensors are mostly used in clinical diagnostics for detecting of biomarkers early, treatment response, disease progression, intravital imaging, and image-guided surgery [9].

Due to the line-like fluorescence emission spectra of lanthanide metal complexes can be altered by altering the coordination environment, lanthanide metal complexes are ideal for use as luminescence probes. In addition, their fluorescent lifetimes are extraordinarily long, measured in milliseconds (3-10 ms) as opposed to nanoseconds (9-10 ns), as is the case with other organic species that are fluorescent.

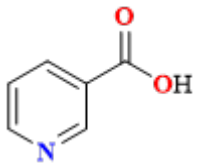

Figure 2: Chemical structure ofNicotinic acid

Titration with an oxidant solution is the traditional method of determining ascorbic acid: dichlorophenol and indophenol [10] and potassium iodate [11]. Liquid chromatography and other chromatographic techniques [12], particularly HPLC with electrochemical detection [13–15], were utilized in the measurement of ascorbic acid in biological fluids and foods. Under pH control, a fluorimetric technique based on the reaction of o-phenylene diamine with dehydroascorbic acid [16, 17], and UV-VIS determinations [18] were utilized as well. ascorbic acid reaction with hexacyanoferrate(III) was the basis for its spectrophotometric evaluation [19] on its oxidation with the Cu(II)-neocuproine complex [20]. Chemiluminescence is another optical method for estimating vitamin C. [21]. Potentiometric, voltammetric, and amperometric methods have all been used to perform electrochemical ascorbic acid determinations. C. E. Langley et al., N. B. Li et al., S. Thiagarajan et al., and A. M. Pisoschi et al. use the voltammetric (CV) technique to give different detection limits (0.01, 0.0004 0.0090, .023, 0.062) mmol L-1, respectively [22–25]. The linear scan voltammetric and second order derivative linear scan voltammetric determination of ascorbic acid with a limit of detection of 3 x10^{-4}, 8 x10^{-4} mmol $L^{-1}$was achieved by A. A. Behfar et al. [26, 27]. Nanoparticles of gold are enhanced with glassy carbon electrodes and worked as a transducer to detect ascorbic acid using the voltammetric (DPV) technique and give LOD = 0.09 and 2×10^{-3} mmol L^{-1} [28, 29]. Glassy carbon electrode improved with poly(bromocre sol purple [30], palladium nanoparticles supported on graphene oxide [31], chitosan incorporating acetyl pyridine bromide [32], polyaniline doped with silicotungstic acid [33] , carbon-supported PdNi nanoparticles and carbon nanotubes electrode [34] transducers used to provide a limit of detection in the range of 6×10^{-3} - 8.0×10^{-4}, mmol L^{-1}.

In this effort, a fluorescence complex with very low value of detection limit and a wide linear range was created for the purpose of detecting ascorbic acid in pharmaceutical ingredients.

2. Material and method

2.1. Chemicals and reagents

All chemical reagents and solvents employed for the synthesis were of analytical grade. In their pure form, nicotinic acid **(figure 2)** was obtained from Aldrich and used without additional purification. All metal salts were purchased from Aldrich. HPLC methanol was used as a synthesis solvent and purchased from Merk. Double-distilled water was used to prepare the solution and for rinsing the critical apparatus, and they were dried in the oven before being used.

2.2. Preparation

2.2.1. Synthesis of the Nic-Tb complex

0.123 g of nicotinic acid (1.0 mmol) was completely dissolved in 10 ml of distilled water. $TbCl_3.6H_2O$ solution in water (0.373 g, 1.0 mmol, 10 ml) was gradually added to the nicotinic acid solution during stirring through a slow addition

of ammonium hydroxide till a white-colored precipitate was formed. The white precipitate was obtained by evaporation of the solvent. The precipitate was filtered off, washed then dried under a vacuum.

2.2.2. Preparation of stock solutions

0.00176 g of powdered ascorbic acid was dissolved in 10 ml of bidistilled water to prepare stock solution of ascorbic acid of 1mM concentration, respectively. Ascorbic acid detection is performed by the Nic-Tb complex of a stock solution of 1mg solid complex in 5ml of bidistilled water ($3.9x10^{-4}$M).

2.3. Method

Fluorescence measurements are performed for the Tb(III) solid complex at an analytical emission wavelength (λ_{em} = 270 nm) of the complex in water. Fluorescence measurement for the interaction of 3.9 $x10^{-6}$M Nic-Tb complex with different concentrations of ascorbic acid in water The study was completed by decreasing of luminescence intensity due to this influence and the quenching that results from the interaction of the Tb(III)-(Nic) probe and ascorbic acid.

2.4. Calculation

Using the Stern-Volmer (1) and Lineweaver-Burk (2) equations, we verified the fluorescence data at different temperatures to prove the quenching process. Most of the time, the two equations are used to explain quenching that is dynamic and static.

$$\frac{F_0}{F} = 1 + K_q \tau_0 \, [Q] = 1 + K_{SV} \, [Q] \qquad (1)$$

where the fluorescence of intensities are $\mathbf{F_0}$ and $\mathbf{F}$, respectively, both when the quencher is present and absent; The constant for the bimolecular quenching rate is $\mathbf{Kq}$;τ_0 is the lifetime of the fluorophore without a quencher; **[Q]** is the concentration of the quencher; Furthermore, the slope can be used to determine **Ksv**, which is the Stern–Volmer quenching constant.

$$(F_0 - F)^{-1} = F_0^{-1} + K_{LB}^{-1} \, . \, F_0^{-1} \, [Q]^{-1} \qquad (2)$$

$\mathbf{K}_{LB}$ is the effective quenching constant for the accessible fluorophores.

According to the effect temperature, the van-t-Hoff plots are being used to examine the thermodynamic parameters. The van't Hoff formula can be used to determine both the change in enthalpy ($\Delta\mathbf{H}°$) and the change in entropy ($\Delta\mathbf{S}°$) if the enthalpy change ($\Delta\mathbf{H}°$) does not significantly change in the temperature range being studied:

$$Ln\, K = \frac{-\Delta H}{RT} + \frac{\Delta S}{R} \qquad (3)$$

From the linear relationship between ln K and the reciprocal absolute temperature, the values of $\Delta\mathbf{H}$ and $\Delta\mathbf{S}$ can be calculated. The following equation is used to determine the value of the free energy change ($\Delta\mathbf{G}°$):

$$\Delta G° = -RT \; lnK \qquad (4)$$

$$\Delta G = \Delta H - T\Delta S \qquad (5)$$

K is the associative binding constants and **R** is the gas constant.

The formula below was used to determine the limit of detection: **LOD = 3.30** σ **/ S**

The following formula was used to determine the limit of quantitation: **LOQ = 10** σ **/ S**

σ**:** residual standard deviation of the regression line.

S: the slope of the regression line.

3. Results and discussion

3.1. Characterization of metal complexes

3.1.1. Stoichiometric analysis

The interaction between Tb(III) ions and nicotinic acid gives a white complex with the formula [Tb $(C_6H_4NO_2)(NH_3)_3(H_2O)_2]Cl_2.3H_2O$, which did not melt until 280 ^oC. The resulting complex was stable in air and soluble in water, methanol, and DMSO. The conductivity value indicates the electrolytic nature of the complex. The physical properties and analytical data CHN% of metal complexes were summarized in **Table 1**.

The Tb-Nic complex has the molecular formula $C_6H_{25}TbN_4O8Cl_2$, the calculated value of carbon was 14.09 %, and the observed value was 14.07 %.

Table 1: Thephysical properties, analytical data CHN% metal complexes

Compound	Molecular weight	Colour	Melting point (°C)	Conductivity (ohm^{-1} cm^2 mol^{-1})	C % Found (calc.).	H% Found (calc.).	N% Found (calc.).
$[Tb(Nic)(NH_3)_3(H_2O)_3]$ $Cl_2.3H_2O$	610.83	White	> 280	82	14.07 (14.09)	4.59 (4.89)	11.14 (10.96)

The calculated value of hydrogen was 4.89 %, and the observed was 4.6 %; for nitrogen, the calculated value was 10.9 % and the observed was 11.14 %. The elemental analysis showed excellent agreement with the calculated values, and the found and calculated values of the percent deviations comply with the accepted limits.

3.1.2. FT-IR Spectra

The broadband at 3675-3112 cm^{-1} could be given as the stretching vibration of the H_2O of nicotinic acid. This band appeared in the Tb-Nic complex, which improved the presence of water of crystalization in the formed complex. The nicotinic acid asymmetric vibration band (COO^-) appeared at 1710 cm^{-1}, while the symmetric bands showed at 1407 cm^{-1}.

The two (COO^-) appeared at 1609 and 1407 cm^{-1} in the formed complex; the $\Delta\upsilon$ were decreased with 100 cm^{-1} from the free ligand, indicating bidentate behavior [35]. The heteroaromatic structure shows the existence of the C–H stretching vibration in the range 3000–3100 cm^{-1}. In the ligand, the C=N stretching vibration appears at 1589 cm^{-1}, but shifts to 1555 cm^{-1} in the complex, showing involvement in the complexation. The complex's (Tb–O) and (Tb-N) weak bands appear at 683 and 548 cm^{-1} [36]. The infrared spectra of the synthesized complexes are shown in **Table 2** and **Figure 3.**

3.1.3. Thermal analysis

The TGA–DTG curves of the thermal decomposition process of the Tb-Nic complex can be divided into three steps (**Figure 4**). In the first step, between 30 - 189°C, there is a mass loss of 6.97 %, which is in good agreement with the value calculated for the release of 3 water for hydration (10.50 %). The sample loses 20.70 % (calcd. 20.50 %) of its initial weight in the sconde step, between 189 - 364°C (**Table 3**). The primary process contains two partly separated decomposition steps related to losing three ammonia and three water molecules from the coordination sphere. Finally, there is a mass loss above 464 °C, which at the first step, but then becomes more gradual, which indicates the gradual decomposition of the nicotinic acid moiety, including the release of $C_2OH_4NCl_2$ from the coordination sphere with a percent of 24.70 % (Calculated. 25.20 %). In the end, rare-earth oxides are the final products; The total mass residue up to 800°C (43.80 %) may include carbon residue, which explains the difference with the theoretical value calculated by taking TbO + 4C as the final product (Calculated. 43.65 %).

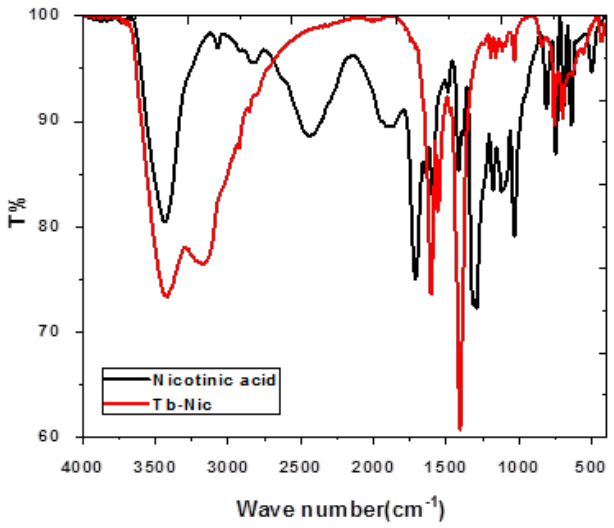

Figure 3: FT-IRspectrum of NiC and Nic-Tb complex

3.1.4. UV Measurement

The complex showed two bands, one at 212 nm and one with three maxima at 256, 263, and 269 nm, assigned to $\pi \rightarrow \pi^*$ and n$\rightarrow \pi^*$ transitions (**Fig-**

Table 2: SignificantIR frequencies (cm^{-1}) for the formed complexes

Ascorbic acid Probe	$(H_2O)/OH$	(COO^-) asymmetric	(COO^-) symmetric	NH_3	M-O	M-N
Free nicotinic acid	3675-3112	1710	1407	-	-	-
$[Tb(Nic)(NH_3)3(H_2O)_2]$ $Cl_2.3H_2O$	3426-3155	1609	1407	3198	683	548

Table 3: TGA, DTG, and DTA of the formed complexes

Compound	Temp. range °C	DTG temp.°C	Mass loss % Found	Mass loss % Calc.	Process	Expected products	Residue (Calcd.) Found
[Tb	30-187	60.2	6.97	7.30	Dehydration	$2H_2O$	TbO+4C
$(Nic)(NH_3)_3(H_2O)_3]$	187-474	209	21.45	20.01	Coordination	$3NH_3+3H_2O$	(45.10)
$Cl_2.3H_2O$					sphere + ligand decomposition		44.7
	474-676	476	26.84	26.16	Ligand decomposition	$C_2OH_4NCl_2$	

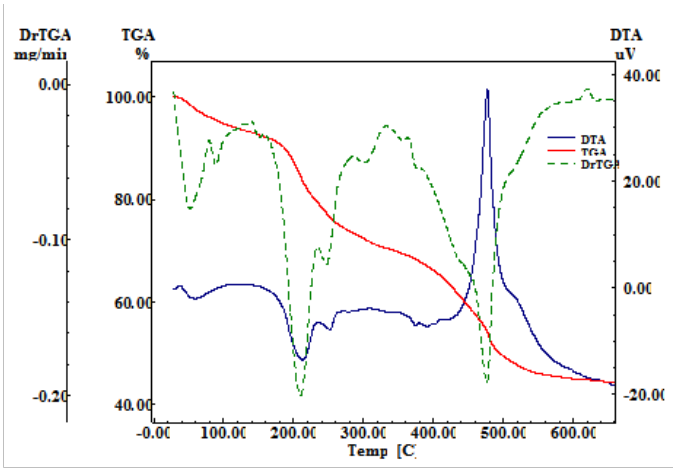

Figure 4: TG/ DTG and DTA curves of Tb_(Nic)complex

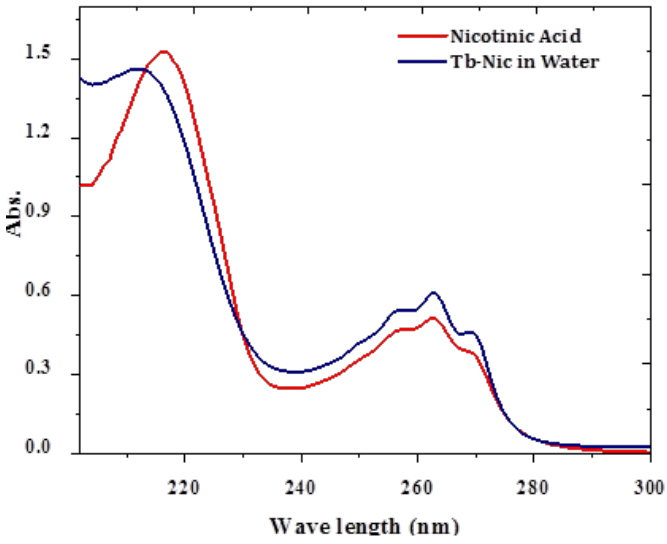

Figure 5: UV-Vis spectrum Nicotinic acid and Tb-Nic complex in water

ure 5).

3.1.5. Solid Fluorescence

The fluorescence spectra of the solid complex have an excitation wavelength of 277 nm a bandwidth of 5 nm and observed emission band at 545nm. The characteristic emission bands of Tb(III) have appeared (**Figure 6**). According to the data above, we have proposed the following structures for the prepared complex, as shown in **(Figure 7)**.

3.2. Fluorescence Mesurément

3.2.1. Effect of time

The emission intensity of the Tb-Nic complex is monitored over time. The data reflect that the complex's fluorescence was fixed for about 60 min-

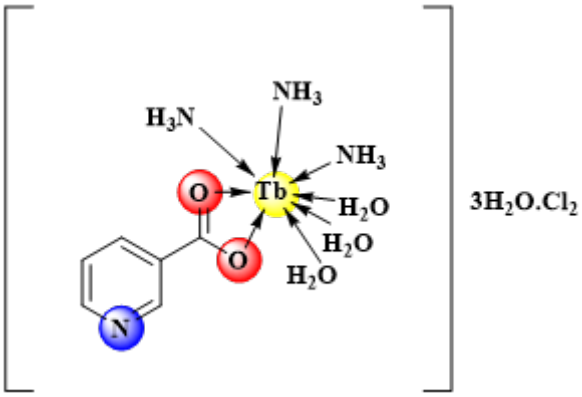

Figure 6: The postulated structures of the prepared complex

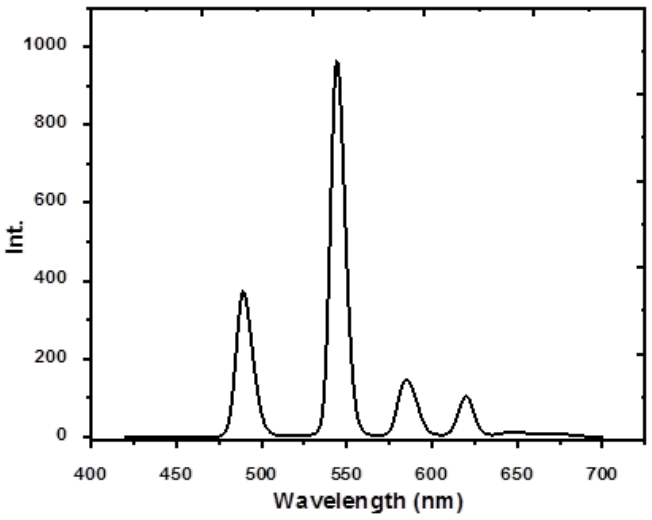

Figure 7: Fluorescence andabsorption spectra of Tb(III)-NIC solid complex

utes, as shown in **Figure 8**. A remarkably sharp decrease was observed after 60 minutes. The measurements using this complex were chosen to be performed, during the first 60 minutes of complex solution preparation.

3.2.2. Effect of solvents

Five solvents have been utilized in our study: protic (distilled water, absolute methanol, and ethanol) and aprotic (acetonitrile and DMSO). The emission spectra of polar fluorophores are profoundly influenced by solvent polarity and the surrounding environment. The solvent effect was achieved by comparing the fluorophore's quantum yields and/or emission spectra when it is attached to the macromolecule and dissolved in solvents of various polarities. The effect of solvent on the fluorescence of the probe is of the following order (**Figure 9**): Methanol > Ethanol > DMSO > Acetonitrile > Water.

3.2.3. Effect of pH

The relationship between pH and Nic-Tb's luminescence intensity is shown in **Figure.10**. The maximum intensity increases as the pH increase from 1.5 to 9.1. The formation of the hydroxo complex or an enhanced intramolecular transfer of charge from the ligand molecule to Tb (III) ions at higher pH values could account for this performance. The intra-molecular energy transfer process may be deactivated by deprotonated nicotinic acid ligands that predominate at lower pH values, resulting in weak fluorescence of the Nic-Tb complex in a medium of high acidity.

3.3. Interaction of Ascorbic acid with the Tb-Nic complex

The spectrofluorometric method was used to investigate the Tb(III)-Nic probe's interaction with ascorbic acid. As shown in **Figure 11**, the complex's luminescence intensity clearly changed (quenching) in the emission intensity. Quenching of the fluorescence indicates that a particular fluorophore's fluorescence intensity is decreased by a number of molecular interactions. [37, 38].

Water was used to obtain the calibration plot for the ascorbic acid assay using the Tb(III)-Nic complex. Ascorbic acid fluorescence measurements of the Tb(III)-Nic complex revealed quenching of the Tb-Nic complex's characteristic peak at 545 nm at different concentrations., as shown in **Figure 12**. The calibration data, correlation coefficient, intercept, and slope are summarized in **Table 4.**

Table 4: Sensitivity and regression parameters (Correlation coefficient, intercept, and slope) for the calibration data

Parameter	Proposed method
Intercept	1
Slope	2.78×10^{3}
Regression coefficient (r)	0.99
LOD	9.1 μM
LOQ	28 μM

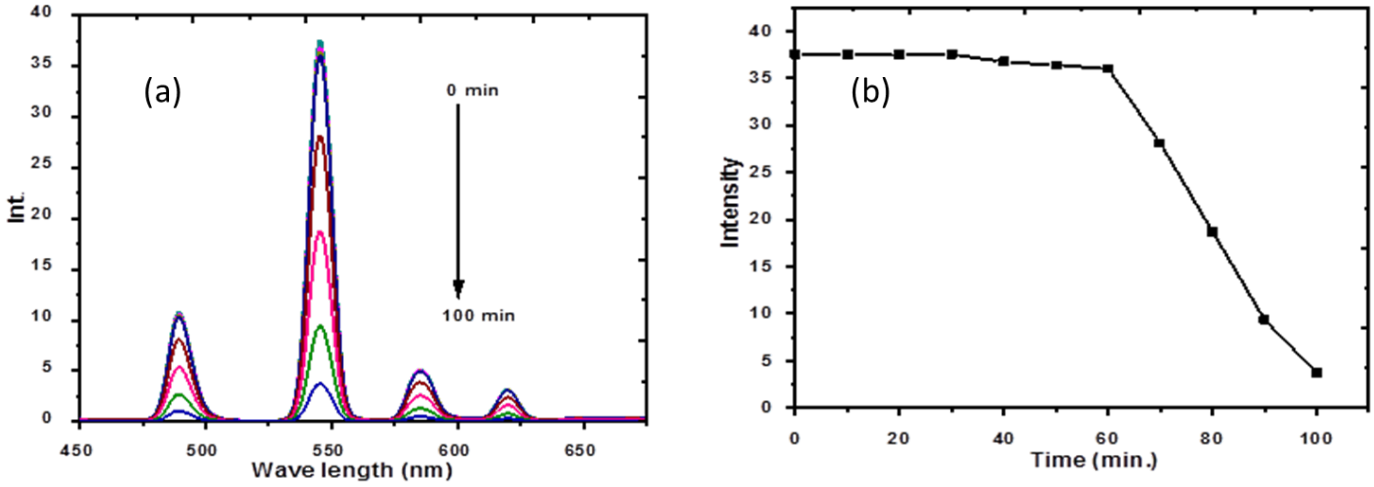

Figure 8: Fluorescence emissionspectra of Tb(III)-(Nic) with time at 545 nm

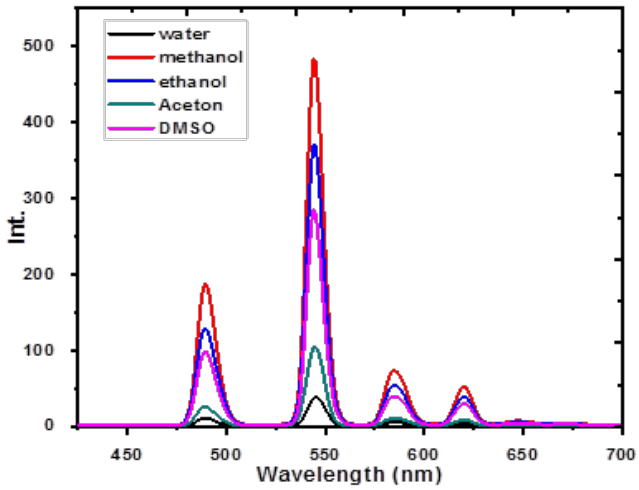

Figure 9: Fluorescence and absorption spectra of Tb(III)-Nic complex in the different solvents at room temperature

3.3.1. *Study of quenching mechanism (Effect of temperature)*

To approve the quenching mechanisms, we used the well-known Stern-Volmer method to examine the fluorescence figures at different temperatures (**see figure 13**).

KD = kqτ_0. yields the Stern-Volmer quenching constant. If the quenching is proven to be dynamic. Otherwise, this constant will be expressed as KSV [39].

According to previous research, the Stern–Volmer curve would be linear over a specific concentration range if the quenching method was single, static or dynamic. [40].

A linear Stern Volmer plot commonly reveals a single class of fluorophores, all similarly within the reach of the quencher. The Stern-Volmer plots deviate from linearity towards the x-axis in the event that there are two fluorophore populations and the quencher is unable to access one of them [39].

Table 5: Fluorescence quenching constant (in the equation of Stern–Volmer) for the interaction between the Nic-Tb complex and ascorbic acid (AA)

Temp (^{o}C)	Stern-Volmer parameters	
	KSV(Lmol^{-l})	R^2
22	3.02×10^3	1
30	3.52×10^3	1
35	3.63×10^3	1
40	3.91×10^3	1
45	4.24×10^3	1

All K_{sv} (L mol^{-1}) of Nic-Tb complex binding with ascorbic acid at different temperatures were calculated in **(Table 5).**

The van't Hoff plots based on the temperature dependence of the binding constant for Nic-Tb - AA binding were used to calculate the thermodynamic parameters in order to confirm the binding

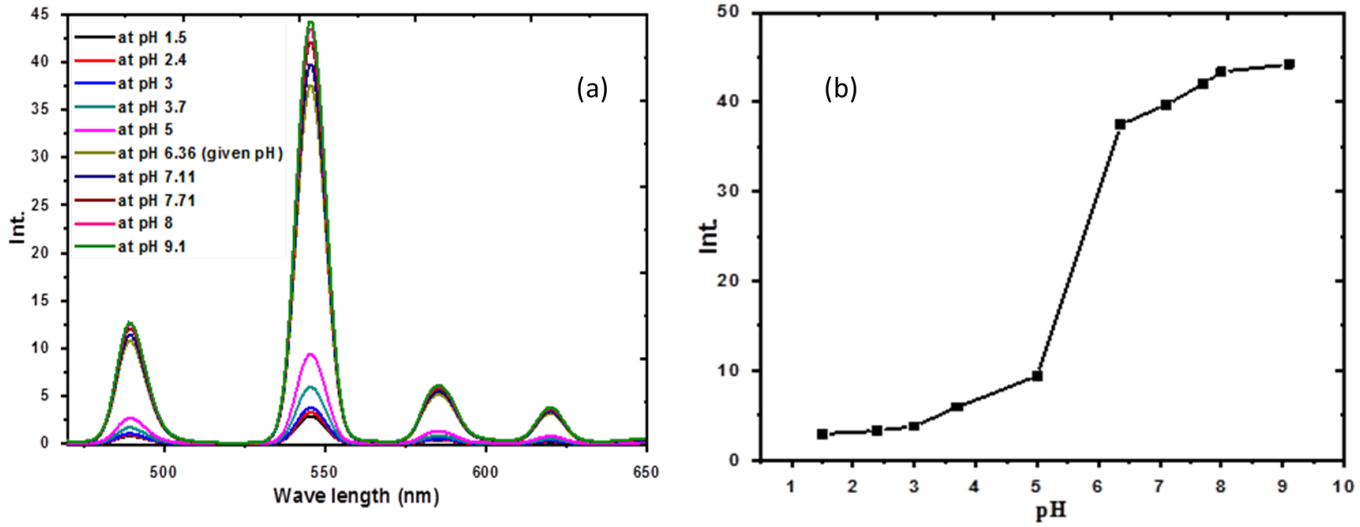

Figure 10: Effect of pH value onluminescence intensity of Tb (III)-Nic complex in aqueous solution

Table 6: Thermodynamic parameters of binding reaction for Nic-Tb complex with ascorbic acid (AA)

Temp (^{o}C)	K (Lmol^{-l})	R^2	ΔH (kJ mol^{-1})	ΔS (J mol^{-1} K^{-1})	ΔG (kJ mol^{-1})
22	2.51×10^3	0.999			-19.21
30	3.52×10^3	1			-20.58
35	3.63×10^3	1	18.0337	126.336	-21.00
40	3.91×10^3	1			-21.53
45	4.24×10^3	1			-22.09

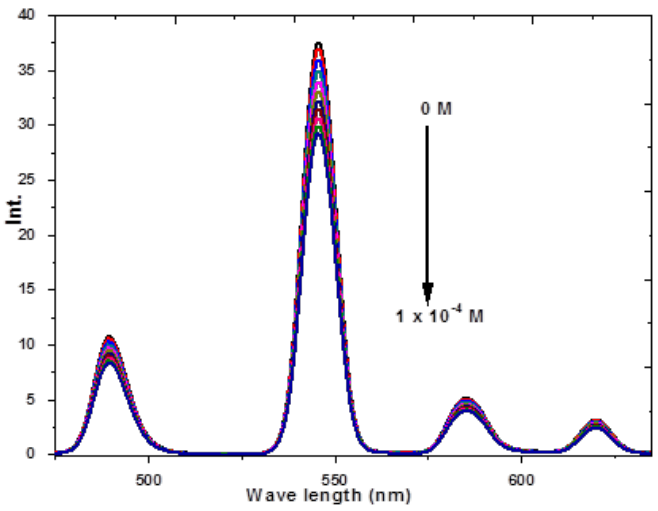

Figure 11: Emission spectra forTb(III)-(Nic)$_3$ complex with ascorbic acid in water at room temperature.

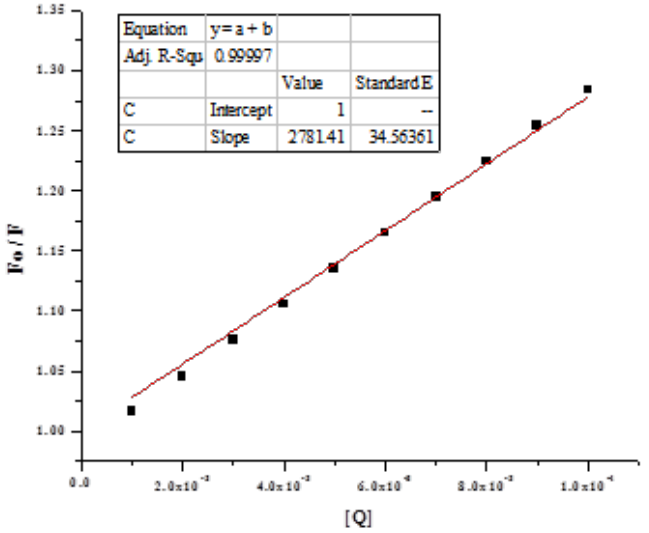

Figure 12: Calibration curve for Tb(III)-Nic complex with different concentrations of Ascorbic acid , in water ,at room temperature

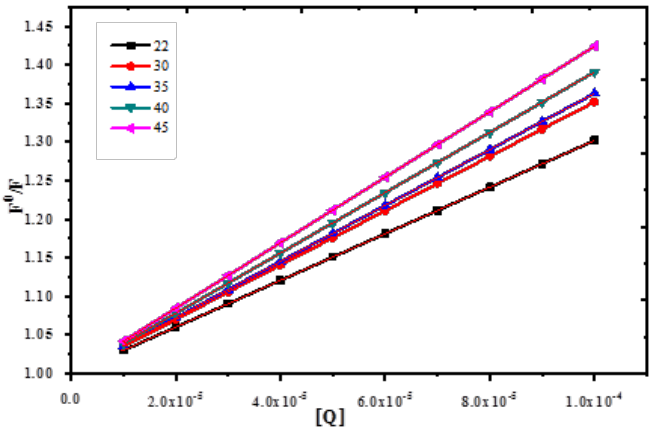

Figure 13: Stern–Volmer plot (F^0/F versus [Q]) of ascorbic acid ([AA] =1×10^{-5}– 1×10^{-4}M) with temperature increasing

mode and clarify the interaction between the complex and the quencher (see **figure 14**).

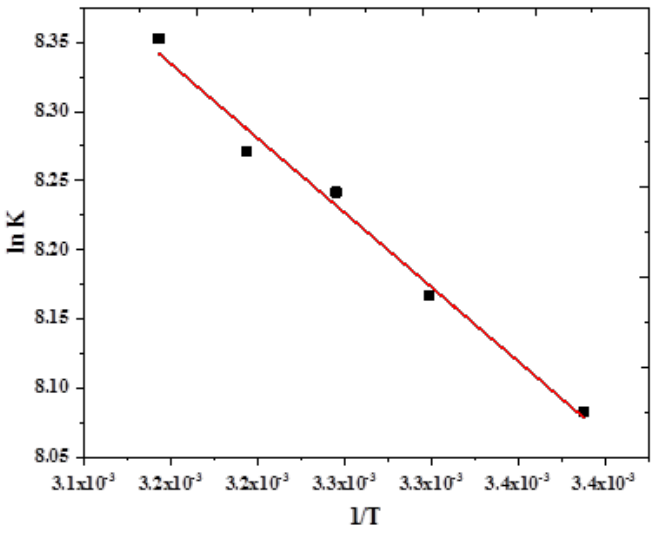

Figure 14: A representative Van't Hoff plot for Tb(III)-Nic-AA binding

The results summarized in **Table 6** show that the Nic-Tb -AA binding cannot be described as a single intermolecular force model. Hypothetically, hydrophobic and electrostatic forces act as the main forces of interaction when $\Delta H^\circ < 0$ or $\Delta H^\circ \approx 0$ and $\Delta S^\circ > 0$, The hydrogen bond and the van der Waals force are the main forces of interaction when $\Delta H^\circ < 0$ and $\Delta S^\circ < 0$. Additionally, hydrophobic interaction takes center stage when ΔH° and ΔS° are greater than 0. Hence, it is probable that hydrophobic is involved in this binding process. Furthermore, we discovered $\Delta G < 0$ for each binding interaction, illustrating that the interaction should be spontaneous.

3.3.2. Effect of interfering species

In the presence of 3×10^{-5} M ascorbic acid, various species of interference were investigated. The tolerance level for interference was set at a fluctuation of (5%) in the average fluorescence intensity at the relevant concentration of ascorbic acid (**Table 7**).

3.4. Application to pharmaceutical drugs:

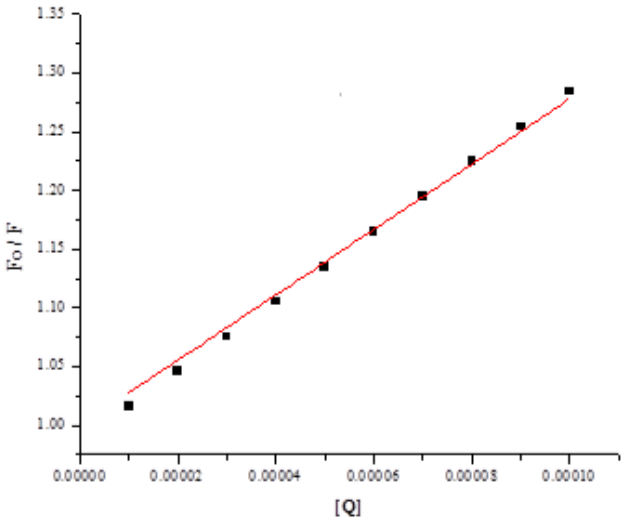

Figure 15: Calibration curve for Tb(III)-Nic complex with different concentrations of Ascorbic acid in water at room temperature. The specified range was derived from linearity studies and was found to be in the range of 1×10^{-5}– 1×10^{-4} M.

Figure 15 shows the calibration curve for determining the optimal reaction conditions of ascorbic acid (Cevarol 500mg/tablet) of pharma top company by its reaction with the Nic-Tb complex which was created by plotting the emission as a function of the analogous concentrations (M). The regression equation of the calibration curve is y = 1 + 2.8 x10^3 X (n=10, R^2= 0.9997).

Table 7: Accuracy of AA analysis.

Sample	Pre-analyzed Product	AA standard addition (M)	Actual AA found (M)	Recovery
1	25 (mg/ml) 0.142 M	1.50×10^{-5}	5.14×10^{-5}	97.60
2		3.50×10^{-5}	8.67×10^{-5}	98.43
3		5.50×10^{-5}	1.22×10^{-4}	98.89

Table 8: Repeatability of AA analysis

Sample	AA actual conc.(M)	AA Found conc.(M)	Mean	SD	RSD (%)
1		3.15×10^{-5}			
2		3.04×10^{-5}			
3	3×10^{-5}	3.03×10^{-5}	3.07×10^{-5}	5.02×10^{-7}	0.0163
4		3.10×10^{-5}			
5		3.07×10^{-5}			
1		5.15×10^{-5}			
2		5.14×10^{-5}			
3	5×10^{-5}	5.20×10^{-5}	5.18×10^{-5}	4.26×10^{-7}	0.00823
4		5.16×10^{-5}			
5		5.25×10^{-5}			
1		7.14×10^{-5}			
2		7.14×10^{-5}			
3	7×10^{-5}	7.18×10^{-5}	7.16×10^{-5}	2.07×10^{-7}	0.0029
4		7.19×10^{-5}			
5		7.15×10^{-5}			

The specified range was discovered through linearity studies to be in the range of 1×10^{-5}–1×10^{-4}M.

The accuracy of the method for adding concentrations was determined by the recovery studies. The recovery values was accurate ranged from 97.6-98.89 (**Table 7**).

The intra-assay precision of the method was established on samples of drug solutions at different concentration levels (**Table 8**) by determining five replicates of each sample as a batch in a single assay run. RSD was less than 0.0163 percent, proving the excellent precision of the technique.

According to the residual standard deviation of the regression line (0.7845) and the slope (2.78×10^{3}), the detection limit was 9.1×10^{-6}M and the quantitation limit was 2.820×10^{-5}M.

3.5. Comparison with other study

Although a lot of research work related to ascorbic acid detection has been reported, there are no commercial sensors of AA available in the market. Our probe has a comparable LOD with other techniques has been used, with a fast, easy and cheap method.

4. Conclusion

A cheap, rapid, accurate, economical, user-friendly, and percise technique for the detection of ascorbic acid using, a Tb(III)-Nic probe has been established with a limit of detection 9 μM. This work investigated the nature of the interaction between the Tb(III)-Nic probe and ascorbic acid. Ascorbic acid in water clearly reduces the fluorescence of Tb(III)-Nic. The calculations reveal

that the probe fluorescence's probable quenching mechanism was dynamically quenched. The thermodynamic parameters showed that the binding was a spontaneous and exothermic process, and as that the corresponding quenching constants increased with temperature. According to the values of the thermodynamic parameters, the binding of Tb(III)-Nic to ascorbic acid is significantly influenced by interactions of electrostatic nature. The complex was synthesized and characterized using different analysis techniques in this work. Our future efforts to develop luminescent lanthanide sensors based on our Tb(III) luminescent complexes will aim to improve sensor selectivity.

References

[1] C. Erdurak-Kiliç, Anodic voltammetric behavior of ascorbic acid and its selective determination in pharmaceutical dosage forms and some Rosa species of Turkey, Journal of Analytical Chemistry 61 (11) (2006) 1113–1120.

[2] S. J. Padayatty, Vitamin C as an antioxidant: evaluation of its role in disease prevention, Journal of the American college of Nutrition 22 (1) (2003) 18–35.

[3] H. Wang, E. Nakata, I. Hamachi, Recent progress in strategies for the creation of protein-based fluorescent biosensors, ChemBioChem 10 (16) (2009) 2560–2577.

[4] M. C. Morris, Fluorescent biosensors of intracellular targets from genetically encoded reporters to modular polypeptide probes, Cell biochemistry and Biophysics 56 (1) (2010) 19–19.

[5] M. Wolff, Novel fluorescent proteins for high-content screening (2006).

[6] P. Lang, Cellular imaging in drug discovery, Nature Reviews Drug Discovery 5 (4) (2006) 343–356.

[7] W. S. El-Deiry, C. C. Sigman, G. J. Kelloff, Imaging and oncologic drug development, Journal of clinical oncology 24 (1920) 3261–3273.

[8] J. K. Willmann, Molecular imaging in drug development, Nature reviews Drug discovery 7 (7) (2008) 591–607.

[9] M. C. Morris, Fluorescent biosensors-probing protein kinase function in cancer and drug discovery, Biochimica et Biophysica Acta -Proteins and Proteomics 1834 (7) (2013) 1387–1395.

[10] S. S. Nielsen, Phenol-sulfuric acid method for total carbohydrates, in Food analysis laboratory manual (2010).

[11] G. Deshmukh, M. Bapat, Determination of ascorbic acid by potassium iodate. Fresenius' Zeitschrift für analytische Chemie (1955).

[12] E. Oliveira, D. Watson, Chromatographic techniques for the determination of putative dietary anticancer compounds in biological fluids, Journal of Chromatography B: Biomedical Sciences and Applications 764 (1-2) (2001) 3–25.

[13] H. Iwase, Use of nucleic acids in the mobile phase for the determination of ascorbic acid in foods by high-performance liquid chromatography with electrochemical detection, Journal of Chromatography A 881 (1-2) (2000) 327–330.

[14] A. Rizzolo, Evaluation of sampling and extraction procedures for the analysis of ascorbic acid from pear fruit tissue. Food Chemistry (2002).

[15] M. Rodrıguez-Comesana, M. Garcıa-Falcón, J. Simal-Gándara, Control of nutritional labels in beverages with added vitamins: screening of β-carotene and ascorbic acid contents. Food Chemistry (2002).

[16] J. Borowski, Content of selected bioactive components and antioxidant properties of broccoli (Brassica oleracea L.). European Food Research Technology (2008).

[17] S. Arya, M. Mahajan, P. Jain, Non-spectrophotometric methods for the determination of Vitamin C, Analytica Chimica Acta 417 (1) (2000) 1–14.

[18] S. Vermeir, Evaluation and optimization of high-throughput enzymatic assays for L-ascorbic acid quantification in horticultural products, Abstracts Biosensors (2008).

[19] T. Lenarczuk, S. Głąb, R. Koncki, Application of Prussian blue-based optical sensor in pharmaceutical analysis, Journal of pharmaceutical and biomedical analysis 26 (1) (2001) 163–169.

[20] K. Güçlü, Spectrophotometric determination of ascorbic acid using copper (II)-neocuproine reagent in beverages and pharmaceuticals, Talanta 65 (5) (2005) 1226–1232.

[21] A. F. Dãnet, M. Badea, H. Y. Aboul-Enein, Flow injection system with chemiluminometric detection for enzymatic determination of ascorbic acid. Luminescence: The journal of biological chemical luminescence (2000).

[22] C. E. Langley, Manganese dioxide graphite composite electrodes: application to the electroanalysis of hydrogen peroxide, ascorbic acid and nitrite. Analytical sciences (2007).

[23] S. Thiagarajan, T. H. Tsai, S. M. Chen, Easy modification of glassy carbon electrode for simultaneous determination of ascorbic acid, dopamine and uric acid, Biosensors and Bioelectronic 24 (8) (2009) 2712–2715.

[24] N. B. Li, W. Ren, H. Q. Luo, Simultaneous voltammetric measurement of ascorbic acid and dopamine on poly (caffeic acid)-modified glassy carbon electrode, Journal of Solid State Electrochemistry 12 (6) (2008) 693–699.

[25] A. M. Pisoschi, Determination of ascorbic acid content of some fruit juices and wine by voltammetry performed at Pt and carbon paste electrodes, Molecules 16 (2) (2011) 1349–1365.

[26] A. A. Behfar, Determination of L-ascorbic acid in plasma by voltammetric method. Iranian journal of pharmaceutical research: IJPR (2010).

[27] P. Deng, Z. Xu, J. Li, Simultaneous determination of

ascorbic acid and rutin in pharmaceutical preparations with electrochemical method based on multi-walled carbon nanotubes-chitosan composite film modified electrode, Journal of pharmaceutical biomedical analysis 76 (2013) 234–242.

[28] J. B. Raoof, Simultaneous voltammetric determination of ascorbic acid and dopamine at the surface of electrodes modified with self-assembled gold nanoparticle films, Journal of Solid State Electrochemistry 14 (7) (2010) 1171–1176.

[29] C. Wang, Simultaneous determination of ascorbic acid, dopamine, uric acid and tryptophan on gold nanoparticles/overoxidized-polyimidazole composite modified glassy carbon electrode, Analytica chimica acta 741 (2012) 15–20.

[30] R. Zhang, Electroanalysis of ascorbic acid using poly (bromocresol purple) film modified glassy carbon electrode. Measurement (2013).

[31] G. H. Wu, An electrochemical ascorbic acid sensor based on palladium nanoparticles supported on graphene oxide, Analytica chimica acta 745 (2012) 33–37.

[32] X. Cao, Simultaneous determination of uric acid and ascorbic acid at the film of chitosan incorporating cetylpyridine bromide modified glassy carbon electrode, Journal of Solid State Electrochemistry 14 (5) (2010) 829–834.

[33] X. Zhang, A glassy carbon electrode modified with a polyaniline doped with silicotungstic acid and carbon nanotubes for the sensitive amperometric determination of ascorbic acid, Microchimica Acta 180 (5-6) (2013) 437–443.

[34] X. Zhang, An electrochemical biosensor for ascorbic acid based on carbon-supported PdNinanoparticles, Biosensors and Bioelectronics 44 (2013) 183–190.

[35] A. A. Taqa, I. A, S. A. Iyoob, Synthesis and characterization of some nicotinic acid complexes, Int. J. Res. Appl. Sci. Eng. Technol 2 (2014) 350–350.

[36] A. Atac, Raman spectra and molecular structure (monomeric and dimeric structures) investigation of nicotinic acid N-oxide: A combined experimental and theoretical study, Spectrochimica Acta Part A: Molecular and Biomolecular Spectroscopy 85 (1) (2012) 145–154.

[37] J. R. Lakowicz, Fluorescence sensing, in Principles of fluorescence spectroscopy (1999).

[38] H. Wang, Fluorescence quenching of 4-tert-octylphenol by room temperature ionic liquids and its application, Journal of fluorescence 23 (2) (2013) 323–331.

[39] P. Mcphie, Principles of fluorescence spectroscopy, Analytical Biochemistry 2 (2000) 353–354.

[40] A. Gong, A fluorescence spectroscopic study of the interaction between epristeride and bovin serum albumine and its analytical application, Talanta 73 (4) (2007) 668–673.